High Power Laser Science and Engineering, (2023), Vol. 11, e2, 7 pages.
doi:10.1017/hpl.2023.7

HIGH POWER LASER SCIENCE AND ENGINEERING

RESEARCH ARTICLE

Demonstration of a petawatt-scale optical parametric chirped pulse amplifier based on yttrium calcium oxyborate

Meizhi Sun[1,2], Jun Kang[1], Xiao Liang[1], Haidong Zhu[1,2], Qingwei Yang[1], Qi Gao[1], Ailin Guo[1], Ping Zhu[1,2], Panzheng Zhang[1,2], Linjun Li[1,2], Lijuan Qiu[1,2], Zhantao Lu[1,2], Sheng Wang[3], Xiaoniu Tu[3], Xinglong Xie[1,2], and Jianqiang Zhu[1,2]

[1] *Key Laboratory on High Power Laser and Physics, Shanghai Institute of Optics and Fine Mechanics, Chinese Academy of Sciences, Shanghai, China*

[2] *Center of Materials Science and Optoelectronics Engineering, University of Chinese Academy of Sciences, Beijing, China*

[3] *Shanghai Institute of Ceramics, Chinese Academy of Sciences, Shanghai, China*

(Received 15 October 2022; revised 29 December 2022; accepted 17 January 2023)

Abstract

As optical parametric chirped pulse amplification has been widely adopted for the generation of extreme intensity laser sources, nonlinear crystals of large aperture are demanded for high-energy amplifiers. Yttrium calcium oxyborate ($YCa_4O(BO_3)_3$, YCOB) is capable of being grown with apertures exceeding 100 mm, which makes it possible for application in systems of petawatt scale. In this paper, we experimentally demonstrated for the first time to our knowledge, an ultra-broadband non-collinear optical parametric amplifier with YCOB for petawatt-scale compressed pulse generation at 800 nm. Based on the SG-II 5 PW facility, amplified signal energy of approximately 40 J was achieved and pump-to-signal conversion efficiency was up to 42.3%. A gain bandwidth of 87 nm was realized and supported a compressed pulse duration of 22.3 fs. The near-field and wavefront aberration represented excellent characteristics, which were comparable with those achieved in lithium triborate-based amplifiers. These results verified the great potential for YCOB utilization in the future.

Keywords: optical parametric amplification; petawatt; ultra-short pulse; yttrium calcium oxyborate

1. Introduction

Extreme intensity light sources are capable of providing a large number of opportunities for natural science in the laboratory, and have been developed rapidly over the last three decades[1,2]. Currently, power up to 10 petawatt (PW)[3,4] as well as the focused intensity of 10^{23} W/cm^2 has been reported[5]. Optical parametric chirped pulse amplification (OPCPA) has been widely adopted in laser facilities, including those installed and proposed[2–17]. The capacity of optical parametric amplifiers as the front-end of those laser facilities, such as gain bandwidth, conversion efficiency, acceptance angle, and walk-off effect, mainly depends on the nonlinear characteristics of the crystals. On the other hand, for master amplifiers, which are featured in high-energy amplification, crystals of large clear aperture and high damage threshold are demanded. As of now, few nonlinear crystals have been used or proposed in high-power laser facilities. Lithium triborate (LiB_3O_5, LBO), with an aperture of approximately 100 mm and a high damage threshold, has supported the OPCPA of multi-PW laser systems centered at 800 nm[9,10]. Deuterated potassium dihydrogen phosphate (KD_2PO_4, DKDP) has been proposed in systems exceeding 10 PW, such as SEL, EXCELS and OPAL, due to two advantages: a large aperture of 400 mm[17] and gain bandwidth over 190 nm at the central wavelength of 910 nm[18–20].

Correspondence to: Xiaoniu Tu, Shanghai Institute of Ceramics, Chinese Academy of Sciences, Shanghai 200050, China. Email: xiaoniu_tu@mail.sic.ac.cn. Xinglong Xie, Jianqiang Zhu, Key Laboratory on High Power Laser and Physics, Shanghai Institute of Optics and Fine Mechanics, Chinese Academy of Sciences, Shanghai 201800, China. Email: xiexl329@mail.shcnc.ac.cn (X. Xie); jqzhu@mail.shcnc.ac.cn (J. Zhu).

In recent decades, there have been vigorous researches on pure yttrium calcium oxyborate (YCOB) and rare-earth-doped YCOB crystals for utilization in parametric processes for three main reasons. Firstly, numerical analysis predicted good phase matching properties with YCOB crystals[21,22]. Experiments with small aperture YCOB crystals have been reported for the validation of parametric performances. Galletti *et al.*[6] reported an optical parametric amplifier with gain bandwidth of more than 200 nm with YCOB crystals of several millimeters in length. Our previous work experimentally demonstrated in a moderate optical aperture of approximately Φ8 mm that YCOB was capable of exhibiting comparable OPCPA performance with beta barium borate (BBO) at 808 nm, and a pump-to-signal conversion efficiency of 40% was achieved with a total gain of approximately 10^9[23]. A novel conception named quasi-parametric amplification (QPA) was proposed and experimentally demonstrated based on Sm^{3+}-doped YCOB crystal (Sm:YCOB) in 2015 by Ma *et al.*[24]. The highest pump-to-signal conversion efficiency of 56% was realized recently by QPA with a Sm:YCOB crystal of 80 mm in length[25]. The works above confirm that YCOB crystal has a great prospect for ultra-intense ultra-short laser pulse generation. Secondly, YCOB can be grown to a large size of approximately 130 mm in diameter, leading to an available aperture of 100 mm × 100 mm to support high-energy amplification[26,27]. The first joule-level OPCPA with YCOB of 63 mm × 68 mm at 800 nm was demonstrated in 2012, and an amplified pulse of 3.36 J was produced[28]. Thirdly, owing to the remarkable thermal properties, such as large temperature acceptance, high thermal conductivity and low coefficient of thermal expansion, YCOB has potential for high average repetition rate laser systems[29]. At present, crystals adopted in optical parametric amplifiers for PW-scale delivery capacity are restrained to LBO and DKDP[9,10,11,16,30]. In this paper, we presented a YCOB-based parametric amplifier based on the SG-II 5 PW laser facility and, for the first time, realized compressed pulses exceeding 1 PW peak power with YCOB crystal.

2. Experimental details

2.1. Experimental setup and incidence laser

The schematic of the experiment, based on the SG-II 5 PW laser facility, is presented in Figure 1. The incidence signal pulses are originally generated by a commercial Ti:sapphire mode-locked oscillator. A small portion of the pulse chain is used as a trigger for the electronic synchronization system, which ensures synchronization accuracy of 14 ps root mean square (RMS) for OPCPA-I and 100 ps RMS for OPCPA-II. The majority of the seed pulses are stretched by an Öffner stretcher, delivered into a pre-compressor and amplified by the preamplifier. A chromatic aberration pre-compensator (CAPC) was installed for pre-compensation of the chromatic aberration deriving from the large aperture transmission spherical elements in the spatial filters (SFs), SF3, SF4 and SF5. It was aligned before SF3 and the capability of high enhancement on the focusing characteristics at the target was verified[31]. The seventh beam of the SG-II facility was used as the pump for the PW-scale amplifier, where the YCOB crystal was located. The high-energy chirped pulse after amplification was delivered into the adaptive optics (AO), by which the wavefront was measured by a Hartmann sensor and corrected by a deformable mirror. Finally, the chirped pulse was injected into the master compressor, after which the compressed pulse was measured with the entire diameter by a home-made autocorrelator.

Compared with the entire system illustrated in Ref. [9], several changes were made for a better performance. The pre-compressor, which was aligned in a Treacy configuration for high-order dispersion control, was moved after the Öffner stretcher, because energy loss deriving from the degradation of the transmission efficiency of the gratings was intolerable when located after OPCPA-I. The grating pairs in the pre-compressor also provided negative linear component dispersion (group velocity dispersion, GVD), and the chirped ratio of seed pulses injected into OPCPA-I at present was deduced to be 21.3 ps/nm, while the energy per pulse was

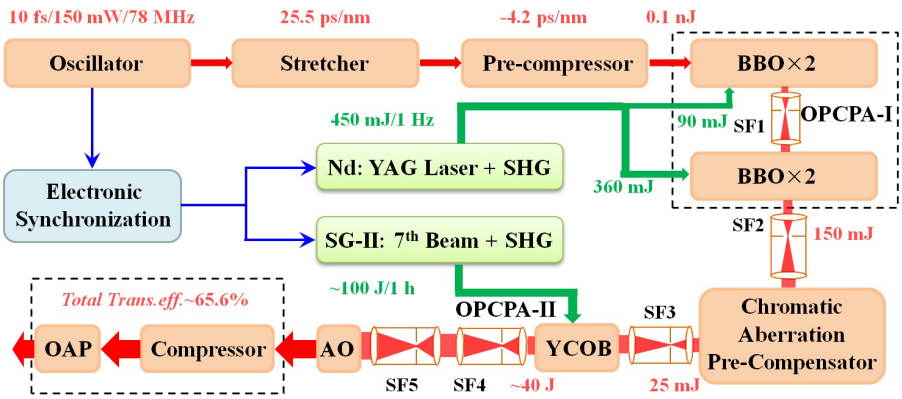

Figure 1. Schematic of the experiment. SHG, second harmonic generation; AO, adaptive optics; OAP, off-axis parabolic mirror.

https://doi.org/10.1017/hpl.2023.7 Published online by Cambridge University Press

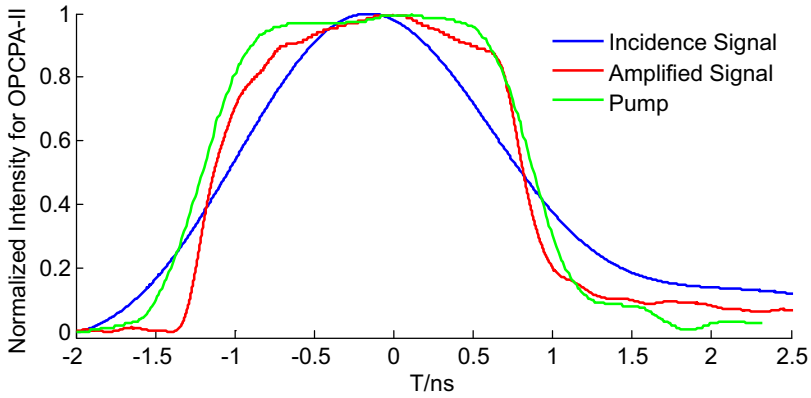

Figure 2. Normalized waveforms of the incidence signal (blue), amplified signal (red) and incidence pump (green) for OPCPA-II.

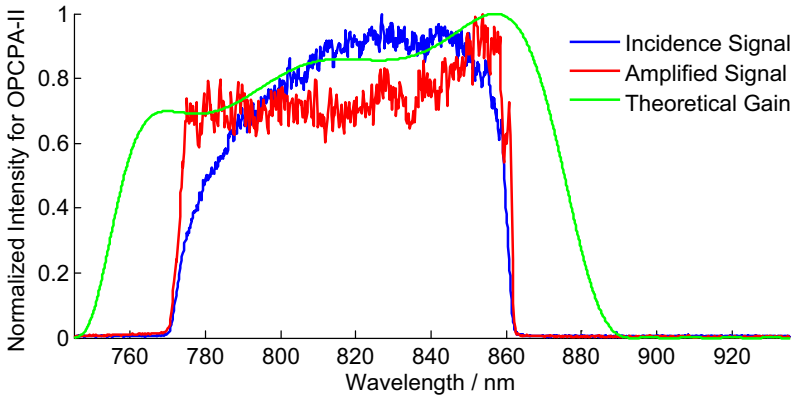

Figure 3. Normalized spectra of the incidence (blue) and amplified (red) signal, compared with the theoretical gain of YCOB-based OPCPA-II (green).

reduced to approximately 0.1 nJ. The pump for OPCPA-I was provided by the Nd:YAG laser, which delivered pulses of 450 mJ in 2.2 ns duration at 532 nm with 1 Hz repetition rate, and four BBO crystals were aligned as before[32]. In our previous work, the pump energy allocation for the prior and the lateral two BBO amplifiers was set (52 and 398 mJ) for optimizing the temporal contrast in pure nanosecond amplifiers[33]. However, in the current condition the injected chirped signal pulse energy was half that of before, so the pump energy allocation was reset (90 and 360 mJ) to ensure a delivery capacity of 150 mJ. The lower energy seed and high-energy pump would degrade the contrast. The waveform and spectrum of the signal pulse after OPCPA-I are represented by the blue lines in Figures 2 and 3, respectively. With a smaller chirped ratio, a broader spectrum bandwidth was temporally overlapped by the pump pulse, and the amplified signal pulse was in the spectrum ranging from 770 to 860 nm and with temporal duration of approximately 1.8 ns. The SFs for image relay were used as before[9]. However, owing to the reflection on 25 element surfaces and bulk losses in the polarized beam splitter (PBS) in the CAPC[31], the total transmission efficiency was limited to approximately 17% and a chirped pulse of approximately 25 mJ was injected into OPCPA-II. The signal after the CAPC was image relayed and beam expanded to Φ90 mm by SF3 to ensure that the pump and signal can be well spatially overlapped.

A thicker crystal as well as higher pump peak power was required to realize a delivery capacity of tens of joules. The duration of the pulse from the seventh beam of the SG-II facility was 2.1 ns and the energy was around 125 J at 1053 nm. The beam aperture was measured as approximately 60 mm square. A large aperture potassium dihydrogen phosphate (KDP) crystal was installed for second harmonic generation and the optimal conversion efficiency was about 80%. Those specifications above ensured a pump pulse of energy of approximately 100 J and intensity of approximately 1.3 GW/cm^2 for OPCPA-II. The waveform of the pump, measured by a phototube and oscilloscope (Tektronix TDS694C), is presented by the green line in Figure 2.

A non-collinear geometry based on YCOB crystal was adopted in OPCPA-II. The crystal was phase-matched at ($\theta = 26.37°, \varphi = 180°$) in the type-I phase matching configuration with an internal non-collinear angle of 2.74°. The non-collinear configuration was set in the *XOZ* principal plane with an effective nonlinear coefficient d_{eff} of approximately 0.95 pm/V because a much larger gain bandwidth can be theoretically achieved than that achieved out of principal

https://doi.org/10.1017/hpl.2023.7 Published online by Cambridge University Press

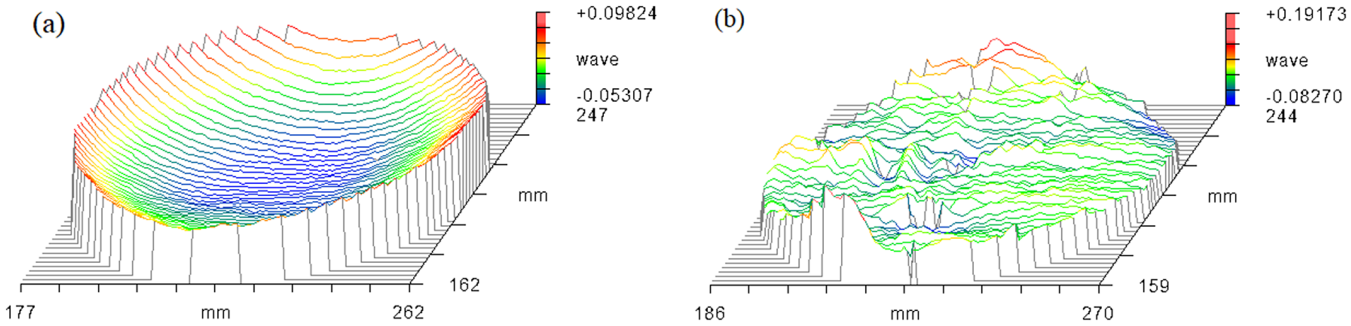

Figure 4. The reflection (a) and transmission (b) properties of YCOB crystal measured by a ZYGO interferometer.

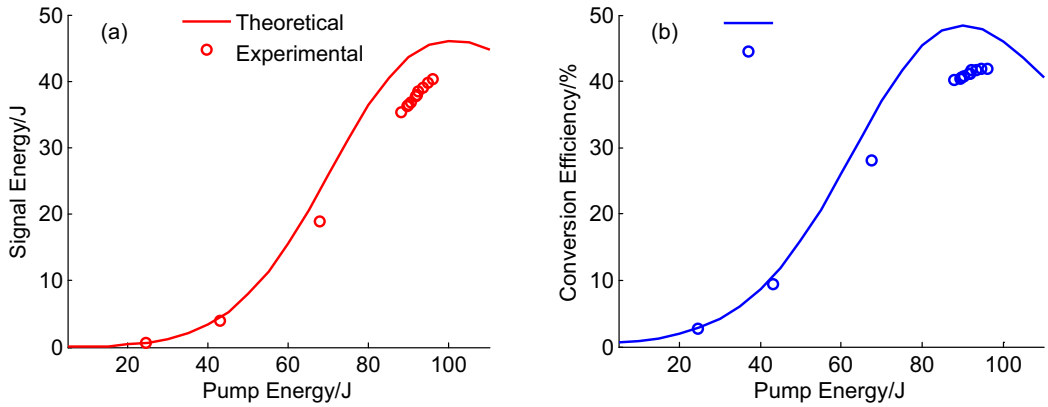

Figure 5. (a) Amplified signal energy achieved by numerical simulation (red solid line) and measured in the experiment (red circles); (b) conversion efficiency obtained by numerical simulation (blue solid line) and experimental measurement (blue circles).

planes with d_{eff} of approximately 1.4 pm/V[22,25]. Numerical simulation based on coupling wave equations was carried out with the parameters of both incident laser pulses and phase-matching conditions[9]. It indicated an optimal crystal length of 27 mm to realize a high gain as well as stability. The normalized gain curve, presented by the green line in Figure 3, indicated a spectrum ranging from 750 to 880 nm, which was much larger than that of the incident signal.

A YCOB crystal boule, with a size of approximately Φ108 mm × 100 mm, was grown by the Bridgeman method, as reported elsewhere[27]. Based on the phase-matching parameters above, the crystal was oriented and cut into an element at a size of Φ100 mm × 27 mm. A wedge angle of 1° was processed to prevent parasitic oscillation. The two clear surfaces were polished without coating. The reflection and transmission properties were measured by a ZYGO interferometer. As shown in Figure 4, the peak to volley (PV) of the reflection wavefront was 0.15λ in a circular region of Φ85 mm, and the PV of the transmission wavefront was smaller than 0.3λ, which indicated a good material uniformity.

2.2. *OPCPA performance of YCOB crystal*

Numerical simulation, in which the spatial profiles of the signal and pump were assumed to be ideal super-Gaussians, for the signal pulse energy versus pump pulse energy, is represented by the red solid line in Figure 5(a). The maximal amplified signal energy would be up to 46 J in theory, corresponding to pump pulse energy of 100 J. In the experiment, the signal pulse energy was smaller than that in the simulation, shown by the red circles in Figure 5(a). The energy of the signal pulse increased rapidly with pump pulse energy, and the highest energy was 40.3 J when the pump pulse energy was 96 J, which indicated a conversion efficiency of 41.98%. The net gain of YCOB-based OPCPA-II was up to 1600. The pump-to-signal conversion efficiency is also provided by the blue solid line in theory and blue circles in the experiment in Figure 5(b). Maximum conversion efficiency of 42.3% was achieved corresponding to pump energy of 92.3%, and the conversion efficiency remained higher than 40% when the pump pulse energy exceeded 88 J.

It was concluded in Ref. [23] that both the amplified spectrum and output energy were very sensitive to the non-collinear angle. In this experiment, we measured the amplified signal energy and obtained the conversion efficiency by precisely tuning the phase-matching angles with a fixed non-collinear angle. As illustrated in Figure 6, the acceptance angle, referring to the full width at half maximum (FWHM) of the conversion efficiency in practice, could be calculated to be approximately 0.08°, which was larger than the 0.02° achieved in the numerical analysis. For comparison, an

https://doi.org/10.1017/hpl.2023.7 Published online by Cambridge University Press

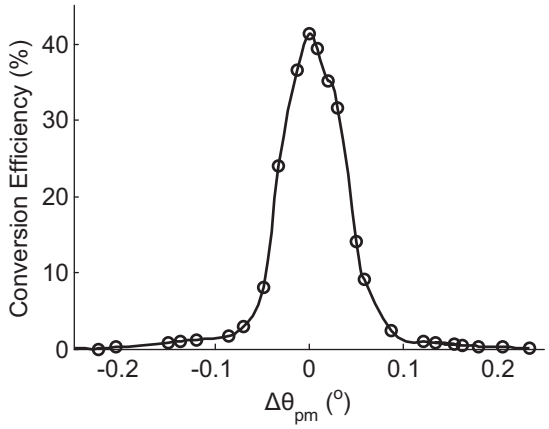

Figure 6. OPCPA conversion efficiency versus the deviation from the optimal phase-matching angle, when the non-collinear angle was set at 2.74°.

acceptance angle of a 19 mm LBO crystal was measured as 0.2° for the same sort of gain levels[9].

The waveform of the amplified signal is represented by red line in Figure 2 and the pulse width was broadened to 1.94 ns, compared with the 1.8 ns of incidence. The pulses for spectrum measurement in our experiment were sampled and attenuated by reflection with optical polished substrate glasses. They were measured by focusing the full-aperture laser beam into a spectrometer (Ocean Optics HR4000+), shown by the red line in Figure 3. A spectrum ranging from 770 to 860 nm was fully amplified in the YCOB-based OPCPA-II with an FWHM spectral bandwidth of 87 nm, which is the largest among PW-scale amplifiers ever reported, to the best of our knowledge[3,4,7,10,12,13,16].

The spatial profile of the amplified signal pulse was measured with an online diagnosis system, sharing the same light path with AO assemblies. It is presented in Figure 7(a); the full aperture was equal to that of the pump beam. For comparison, an experiment using 19-mm-thick LBO crystal was accomplished. To ensure the output energy and conversion efficiency with LBO being the same scale as YCOB, the pump pulse duration was reset to 1.6 ns so that the peak intensity was approximately 2 GW/cm^2, which was still well below the damage threshold of LBO. However, the output bandwidth with LBO was only 75 nm. Figure 7(b) provides the spatial profile of the amplified signal pulse after the LBO-based OPCPA-II for comparison. We used the fill factor (FF) and fluence beam contrast (FBC) to quantitatively describe the near-field distribution characteristics[9]. A numerical analysis showed that the [FF, FBC] were [0.56, 0.12] for YCOB and [0.45, 0.2] for LBO, respectively. The YCOB-based OPCPA was capable of attaining a good near-field distribution, which was comparable to that achieved based on LBO.

To investigate the influence of material uniformity of YCOB crystal presented by the transmission property in Figure 4(b) on the parametric process, the wavefront was measured by the AO system[9]. Wavefront aberration as the static quantity was firstly measured when only OPCPA-I was operated at a 1 Hz repetition rate. After that, it was corrected by the deformable mirror. The shape of the deformable mirror was kept and a new wavefront was measured by the Hartmann sensor when both OPCPA-I and OPCPA-II were operated. The dynamic wavefront aberration derived from the YCOB-based OPCPA–II is shown in Figure 8(a), and the PV and RMS were 2.452λ and 0.388λ, respectively. For comparison, the dynamic wavefront aberration from the LBO-based OPCPA–II is also presented under the same measurement condition, and the PV, RMS values of 2.098λ, 0.351λ were of the same scale as that of YCOB. This indicates a comparable focusing property between YCOB and LBO.

With our home-made second-order autocorrelator[34], the compressed pulse traces after the master compressor were measured and are shown in Figure 9. The sampled pulse for measurement was of the whole beam size of 290 mm × 290 mm. The Gaussian profile fitting showed that the FWHM pulse duration was 22.3 fs. The total transmission

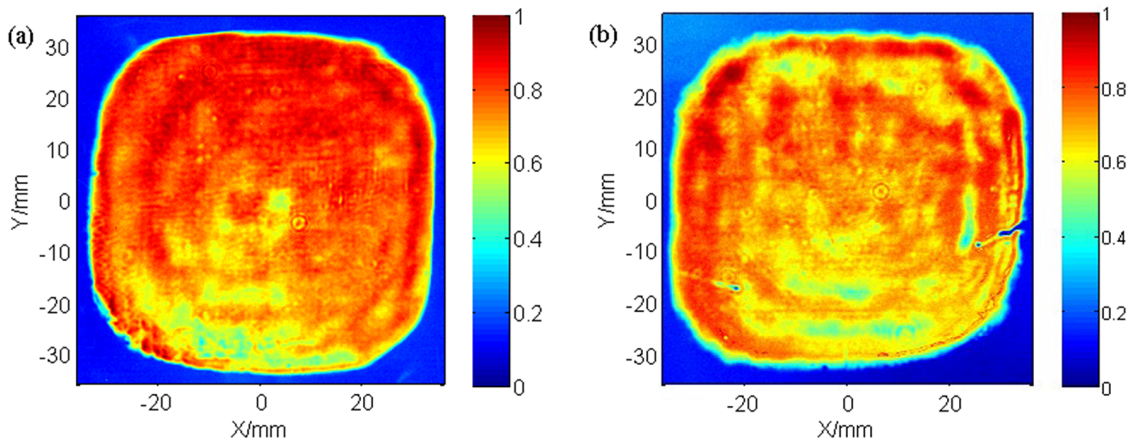

Figure 7. Near fields of the amplified signal in OPCPA-II based on YCOB (a) and LBO (b) crystals.

https://doi.org/10.1017/hpl.2023.7 Published online by Cambridge University Press

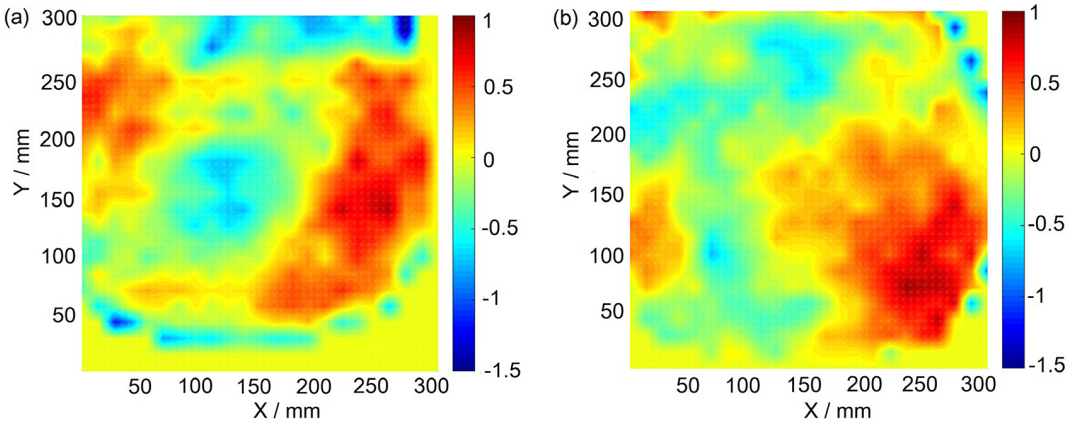

Figure 8. The dynamic wavefront aberrations measured by a Hartmann sensor in the adaptive optics assembly for OPCPA–II with YCOB crystal (a) and LBO crystal (b).

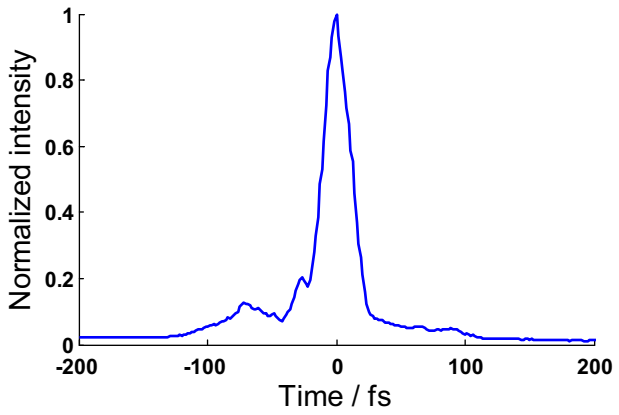

Figure 9. The autocorrelation (AC) trace of a signal pulse after the master compressor.

efficiency of the master compressor and off-axis parabolic mirror (OAP) was measured to be 65.6%, on average. The pulse energy after compression exceeds 26 J and the peak power can be estimated as 1.17 PW.

3. Conclusion

In summary, we reported a high-energy optical parametric amplifier based on YCOB crystal with a diameter of 100 mm. The amplifier was installed at the OPCPA-II stage by replacing the original LBO crystal in the SG-II 5 PW facility platform, and it achieved a good performance. Chirped pulse energy of around 40 J was realized, with a large gain of approximately 1600 and an optimal pump-to-signal conversion efficiency of 42.3%. A spectrum ranging from 770 to 860 nm was almost fully amplified with an FWHM bandwidth of 87 nm. The parametric performance of YCOB was very sensitive to the phase-matching angle and its acceptance angle was about 0.08° in practice. The near-field distribution as well as the wavefront of the amplified signal pulse was measured before compression with the AO system and represented comparable characteristics with those achieved with LBO crystal. A compressed duration of 22.3 fs was measured with the entire beam diameter, indicating a peak power of PW scale. It was the first YCOB-based optical parametric amplifier exceeding 1 PW, to the best of our knowledge. Considering the prominent thermal properties, YCOB crystal has great application prospects for PW laser facilities of high repetition rate in the future.

Acknowledgements

This work was partially supported by the Shanghai Natural Science Foundation (No. 20ZR1464400); the National Natural Science Foundation of China (NSFC) (Nos. 12074399, 12204500 and 12004403); the Key Projects of Intergovernmental International Scientific and Technological Innovation Cooperation (No. 2021YFE0116700); the Shanghai Sailing Program (No. 22YF1455300); the International Partnership Program of the Chinese Academy of Sciences (No. 181231KYSB20170022); the Chinese Academy of Sciences (Nos. CXJJ-21S015, XDA25020311 and XDA25020105); NSAF (No. U1930126).

References

1. G. Mourou and T. Tajima, Science **331**, 41 (2011).
2. C. N. Danson, C. Haefner, J. Bromage, T. Butcher, J. F. Chanteloup, E. A. Chowdhury, A. Galvanauskas, L. A. Gizzi, J. Hein, D. I. Hillier, N. W. Hopps, Y. Kato, E. A. Khazanov, R. Kodama, G. Korn, R. Li, Y. Li, J. Limpert, J. Ma, C. H. Nam, D. Neely, D. Papadopoulos, R. R. Penman, L. Qian, J. J. Rocca, A. A. Shaykin, C. W. Siders, C. Spindloe, S. Szatmári, R. M. G. M. Trines, J. Zhu, P. Zhu, and J. D. Zuegel, High Power Laser Sci. Eng. **7**, e54 (2019).
3. W. Li, Z. Gan, L. Yu, C. Wang, Y. Liu, Z. Guo, L. Xu, M. Xu, Y. Hang, Y. Xu, J. Wang, P. Huang, H. Cao, B. Yao, X. Zhang, L. Chen, Y. Tang, S. Li, X. Liu, S. Li, M. He, D. Yin, X. Liang, Y. Leng, R. Li, and Z. Xu, Opt. Lett. **43**, 5681 (2018).
4. F. Lureau, G. Matras, O. Chalus, C. Derycke, T. Morbieu, C. Radier, O. Casagrande, S. Laux, S. Ricaud, G. Rey, A. Pellegrina, C. Richard, L. Boudjemaa, C. Simon-Boisson, A.

https://doi.org/10.1017/hpl.2023.7 Published online by Cambridge University Press

Baleanu, R. Banici, A. Gradinariu, C. Caldararu, B. De Boisdeffre, P. Ghenuche, A. Naziru, G. Kolliopoulos, L. Neagu, R. Dabu, I. Dancus, and D. Ursescu, High Power Laser Sci. Eng. **8**, e43 (2020).
5. J. W. Yoon, Y. G. Kim, I. Choi, J. H. Sung, H. W. Lee, S. K. Lee, and C. H. Nam, Optica **8**, 630 (2021).
6. M. Galletti, H. Pires, V. Hariton, J. Alves, P. Oliveira, M. Galimberti, and G. Figueira, High Power Laser Sci. Eng. **8**, e29 (2020).
7. H. Kiriyama, A. S. Pirozhkov, M. Nishiuchi, Y. Fukuda, K. Ogura, A. Sagisaka, Y. Miyasaka, M. Mori, H. Saksaki, N. P. Dover, K. Kondo,J. K. Koga, T. Z. Esirkepov, M. Kando, and K. Kondo, Opt. Lett. **43**, 2595 (2018).
8. A. Kessel, V. E. Leshchenko, O. Jahn, M. Kruger, A. Munzer, A. Schwarz, V. Pervak, M. Trubetskov, S. A. Trushin, F. Krausz, Z. Major, and S. Karsch, Optica **5**, 434 (2018).
9. J. Zhu, X. Xie, M. Sun, J. Kang, Q. Yang, A. Guo, H. Zhu, P. Zhu, Q. Gao, X. Liang, Z. Cui, S. Yang, C. Zhang, and Z. Lin, High Power Laser Sci. Eng. **6**, e1 (2018).
10. X. Zeng, K. Zhou, Y. Zuo, Q. Zhu, J. Su, X. Wang, X. Wang, X. Huang, X. Jiang, D. Jiang, Y. Guo, N. Xie, S. Zhou, Z. Wu, J. Mu, H. Peng, and F. Jing, Opt. Lett. **42**, 2014 (2017).
11. J. Bromage, S. W. Bahk, I. A. Begishev, C. Dorrer, M. J. Guardalben, B. N. Hoffman, J. B. Oliver, R. G. Roides, E. M. Schiesser, M. J. Shoup, S. B. Webb, D. Weiner, and J. D. Zuegel, High Power Laser Sci. Eng. **7**, e4 (2019).
12. J. Sung, H. Lee, J. Yoo, J. Yoon, C. Lee, J. Yang, Y. Son, Y. Jang, S. Lee, and C. Nam, Opt. Lett. **42**, 2058 (2017).
13. D. N. Papadopoulos, P. Ramirez, K. Genevrier, L. Ranc, N. Lebas, A. Pellegrina, C. Le Blanc, P. Monot, L. Martin, J. P. Zou, F. Mathieu, P. Audebert, P. Georges, and F. Druon, Opt. Lett. **42**, 3530 (2017).
14. F. Batysta, R. Antipenkov, T. Borger, A. Kissinger, J. T. Green, R. Kananavicius, G. Cheriaux, D. Hidinger, J. Kolenda, E. Gaul, B. Rus, and T. Ditmire, Opt. Lett. **43**, 3866 (2018).
15. E. W. Gaul, M. Martinez, J. Blakeney, A. Jochmann, M. Ringuette, D. Hammond, T. Borger, R. Escamilla, S. Douglas, W. Henderson, G. Dyer, A. Erlandson, R. Cross, J. Caird, C. Ebbers, and T. Ditmire, Appl. Opt. **49**, 1676 (2010).
16. V. V. Lozhkarev, G. I. Freidman, V. N. Ginzburg, E. V. Katin, E. A. Khazanov, A. V. Kirsanov, G. A. Luchinin, A. N. Mal'shakov, M. A. Martyanov, O. V. Palashov, A. K. Poteomkin, A. M. Sergeev, A. A. Shaykin, and I. V. Yakovlev, Laser Phys. Lett. **4**, 421 (2007).
17. X. Cai, X. Lin, G. Li, J. Lu, Z. Hu, and G. Zheng, High Power Laser Sci. Eng. **7**, e46 (2019).
18. C. Skrobol, I. Ahmad, S. Klingebiel, C. Wandt, S. A. Trushin, Z. Major, F. Krausz, and S. Karsch, Opt. Express **20**, 4619 (2012).
19. C. Hernandez-Gomez, S. P. Blake, O. Chekhlov, R. J. Clarke, A. M. Dunne, M. Galimberti, S. Hancock, R. Heathcote, P. Holligan, A. Lyachev, P. Matousek, I. O. Musgrave, D. Neely, P. A. Norreys, I. Ross, Y. Tang, T. B. Winstone, B. E. Wyborn, and J. Collier, J. Phys. Conf. Ser. **244**, 032006 (2010).
20. J. Bromage, S. W. Bahk, M. Bedzyk, I. A. Begishev, S. Bucht, C. Dorrer, C. Feng, C. Jeon, C. Mileham, R. G. Roides, K. Shaughnessy, M. J. Shoup, M. Spilatro, B. Webb, D. Weiner, and J. D. Zuegel, High Power Laser Sci. Eng. **9**, e63 (2021).
21. M. Sun, L. Ji, Q. Bi, N. Wang, J. Kang, X. Xie, and Z. Lin, Chin. Opt. Lett. **9**, 101901 (2011).
22. H. Pires, M. Galimberti, and G. Figueira, J. Opt. Soc. Am. B Opt. Phy. **31**, 2608 (2014).
23. S. Yang, X. Liang, X. Xie, Q. Yang, X. Tu, Y. Zheng, X. Zhang, Y. Zhang, A. Guo, P. Zhu, J. Kang, M. Sun, and J. Zhu, Opt. Express **28**, 11645 (2020).
24. J. Ma, J. Wang, P. Yuan, G. Xie, K. Xiong, Y. Tu, X. Tu, E. Shi, Y. Zheng, and L. Qian, Optica **2**, 1006 (2015).
25. J. Ma, K. Xiong, P. Yuan, X. Tu, J. Wang, G. Xie, Y. Zheng, and L. Qian, Light Sci. Appl. **11**, 269 (2022).
26. X. Tu, S. Wang, K. Xiong, Y. Zheng, and E. Shi, J. Cryst. Growth **488**, 23 (2018).
27. X. Tu, S. Wang, K. Xiong, Y. Zheng, and E. Shi, J. Cryst. Growth **535**, 125527 (2020).
28. L. Yu, X. Liang, J. Li, A. Wu, Y. Zheng, X. Lu, C. Wang, Y. Leng, J. Xu, R. Li, and Z. Xu, Opt. Lett. **37**, 1712 (2012).
29. Z. Liao, I. Jovanovic, C. A. Ebbers, Y. Fei, and B. Chai, Opt. Lett. **31**, 1277 (2006).
30. O. V. Chekhlov, J. L. Collier, I. N. Ross, P. K. Bates, M. Notley, C. Hernandez-Gomez, W. Shaikh, C. N. Danson, D. Neely, P. Matousek, S. Hancock, and L. Cardoso, Opt. Lett. **31**, 3665 (2006).
31. Z. Cui, J. Kang, A. Gu, H. Zhu, Q. Yang, P. Zhu, M. Sun, Q. Gao, D. Liu, X. Ouyang, Z. Zhang, H. Wei, X. Liang, C. Zhang, S. Yang, D. Zhang, X. Xie, and J. Zhu, Opt. Express **27**, 16812 (2019).
32. X. Liang, X. Xie, J. Kang, Q. Yang, H. Wei, M. Sun, and J. Zhu, High Power Laser Sci. Eng. **6**, e58 (2018).
33. M. Sun, X. Xie, J. Zhu, X. Zhang, Y. Zhang, P. Zhu, A. Guo, J. Kang, H. Zhu, Q. Yang, and X. Liang, Appl. Opt. **60**, 2056 (2021).
34. Q. Yang, Z. Cui, J. Kang, A. Guo, H. Zhu, M. Sun, P. Zhu, Q. Gao, X. Xie, and J. Zhu, Opt. Eng. **57**, 064103 (2018).

https://doi.org/10.1017/hpl.2023.7 Published online by Cambridge University Press